Composites Communications 20 (2020) 100348

Contents lists available at ScienceDirect

Composites Communications

journal homepage: www.elsevier.com/locate/coco

Electrospun luminescent piezo webs as self-powered sensing platform for small accelerations at low frequency

Xi Huang [a,1], Long Jin [a,1], Chuanfeng Wang [a], Yali Xu [a], Zhou Peng [a], Meilin Xie [a], Chaoliang Zhang [b], Weiqing Yang [a,**], Jun Lu [a,2,*]

[a] Key Laboratory of Advanced Technologies of Materials, Ministry of Education, School of Materials Science and Engineering, Southwest Jiaotong University, Chengdu, 610031, Sichuan, China

[b] State Key Laboratory of Oral Diseases, West China Hospital of Stomatology, Sichuan University, Chengdu, 610041, China

ARTICLE INFO

Keywords:
Multifuction Integrated composites
Polyvinylidene fluoride
Carbon dots
Electrospinning
Electrical properties

ABSTRACT

The sensitive detection of low frequency small accelerations is particularly desirable in seismic prediction, wave energy utilization and dam/bridge damage monitoring. In this work, we report for the first time the electrospinning of polyvinylidene fluoride/carbon dots (PVDF/CDs) nanofibers and their piezoresponse under different acceleration rate. The desirable nanofibrous mats, with thin and smooth morphology, are acquired by changing spinning parameters, and β-phase crystal content is improved with increasing introduction of CDs. At an acceleration rate of 6 m/s^2, frequency of 1.6 Hz and applied force of 35 N, the maximum open-circuit voltage density of 55.6 V cm^{-3}, and short-circuit current density of 2.1 μA cm^{-3} are achieved for PVDF/CDs fiber with 1% (wt/v) CDs loading. In particular, the fiber mat is tested with detection sensitivity of acceleration change up to 0.4 m/s^2 for potential as an acceleration sensor. Moreover, CDs not only improve the piezoresponse of PVDF fiber, but also endow the substrate with multifluorescence performance. The as prepared fiber could be used as active layer to perceive the prevalent small acceleration changes at low frequency, such as those from earthquake, tidal flow, ocean waves, reservoir dams, railway bridges, and so on.

1. Introduction

As the world entering the era of internet of things (IoTs), miniaturization and clean energy driving have been a promising trend for smart electronics since the power needed is small [1]. After decades of development, self-power has demonstrated applications in sensing, embedded electronics, actuators, etc [2–5]. Among many energy harvesting methods, such as piezo-, pyro-, and tribo-electricity [6–11], piezoelectric materials process a small mechanical movement, excellent stability and diversified design, leading to approach to nano/-microsystems [12]. Specially, polyvinylidene fluoride (PVDF) and its derivatives have inherent flexibility when compared with ceramics, and show the highest piezoelectric coefficients among polymeric materials [6]. However, the development is still confined by the low energy conversion efficiency [6]. Fundamentally, β and γ crystals, contributing most for piezoelectricity with asymmetric crystal structure, are in urgent need of improvement, although α crystal is the most stable in thermodynamics [13].

As the most efficient technique to prepare nanofibers, electrospinning can provide in-situ high electrical field and strong mechanical stretching at the same time [14–16], proven an effective way to facilitate polar β and γ crystal phases. In addition, PVDF fiber with finer uniform structures exhibits superior polarity and facilitates piezoelectricity [17]. On the other hand, nanofillers have been demonstrated a reliable modifying agent for PVDF to improve crystallization [18,19], dielectric property [20,21], and other performance [19,22,23]. With nanoscale aqueous solubility, low toxicity, tunable photoluminescent (PL) and optical properties, carbon dots (CDs) have demonstrated positive influence on the crystallization of PVDF and its derivatives only in a high pressure process [24,25]. Therefore, investigating the effects of CDs on electrospun PVDF fiber is highly desirable and mandatory.

In this study, electrospinning technique was employed to prepare

* Corresponding
** Corresponding
E-mail addresses: wqyang@swjtu.edu.cn (W. Yang), junluprc@hotmail.com (J. Lu).
[1] These authors equally contributed to this work.
[2] Other used names Jun Lv and Jun Lyu.

https://doi.org/10.1016/j.coco.2020.04.014
Received 28 March 2020; Received in revised form 21 April 2020; Accepted 22 April 2020
Available online 29 April 2020

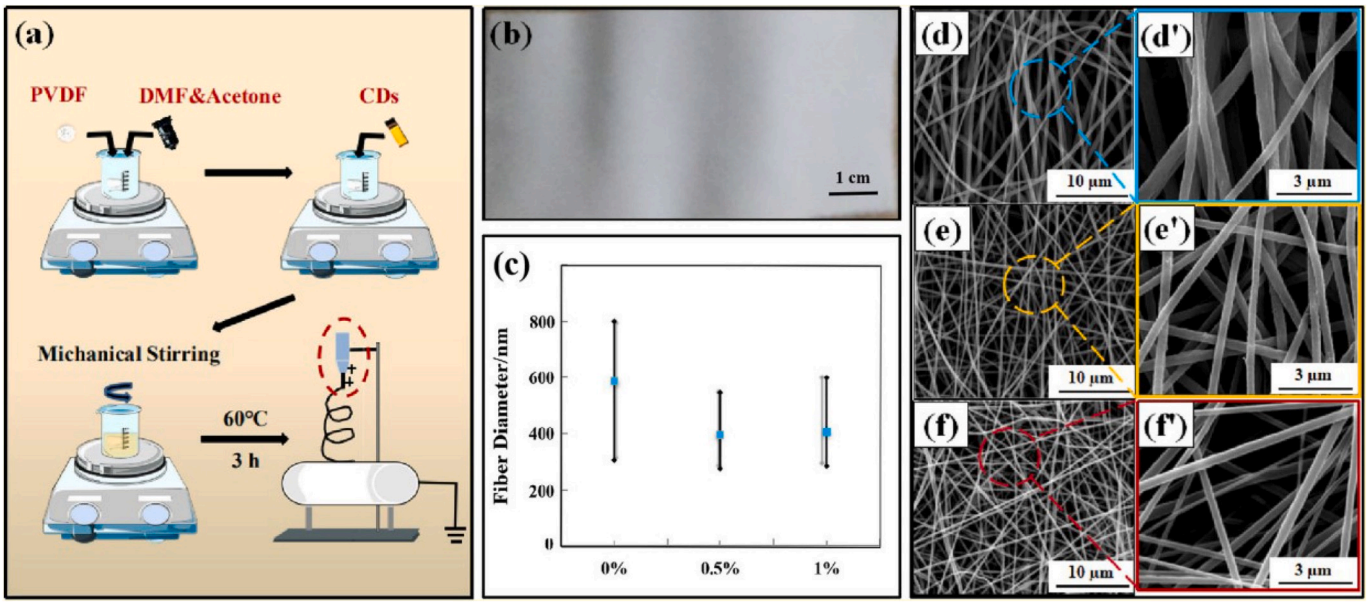

Fig. 1. (a) Illustration of fiber preparation process. (b) Photograph of electrospun PVDF fiber mat. (c) Statistical diagram of fiber diameter and (d–f) SEM images of electrospun PVDF/CDs fiber with different CDs loading. (d'-f') Partial enlargements of (d–f).

PVDF/CDs nanofibers for the first time. Spinning parameters were adjusted to obtain desirable PVDF nanofiber with thin and smooth morphology, since fine fiber morphology exhibits better mechanical-to-electrical conversion [12]. Adding CDs further reduced fiber diameter and enhanced piezoelectricity. Consequently, PVDF/CDs fiber with 1% (wt/v) CDs loading delivered maximum open-circuit voltage density of 55.6 V cm^{-3}, and short-circuit current density of 2.1 μA cm^{-3} at an acceleration rate of 6 m/s^2, frequency of 1.6 Hz and applied force of 35 N. Besides, CDs also endowed nanofiber with multicolor fluorescent performance. The as prepared flexible, skin-friendly PVDF/CDs nanofibers can be utilized in wearable energy supply devices for detecting bodily functions like heartbeat or movements. And more significantly, they promise applications in self-powered sensing for seismic prediction, tidal and wave energy utilization, and dam/bridge damage monitoring. This work may benefit the development of polymeric based piezoelectric composites with integrated functions.

2. Experimental

2.1. Materials

CDs were supplied by Janas New-Materials Co., Ltd, China, with a diameter of around 5 nm. The PL emission spectra of CDs, under different excitation lights, are shown in Fig. S1. PVDF of $M_w = 322\,000$ g mol^{-1} was provided by Solvay Co., Ltd., Belgium. N, N-dimethylformamide (DMF) and acetone were purchased from Chengdu Kelong Chemical Co., Ltd, China.

2.2. Preparation of PVDF/CDs composite nanofibers

Electrospinning solutions were acquired by dissolving PVDF powder and CDs into a mixture solvent of DMF and acetone at 60 °C for 3 h. After resting for 30 min, the defoamed solution was gradually cooled to room temperature and shifted into a 20 mL syringe. Nanofiber mats were produced using a needle based electrospinning setup. Solvents constituents, electrical bias, polymer concentration and CDs content were changed for fine fiber morphology. Injection rate was fixed at 1 mL/h to maintain a stable spinning condition. The fiber was collected by an aluminum roller drum, with a diameter of 5 cm and length of 10 cm, and with rotating speed of 1200 r/min. Spinning time lasted for 12 h, and fiber thickness was measured with a digital micrometer.

2.3. Characterizations

Fiber morphology was observed with a scanning electron microscopy (SEM, JSM-6330F). Differential scanning calorimetry (DSC) measurements were conducted with a TA-Q20 instrument under a N_2 atmosphere protection. Each sample weighed around 6–8 g and was heated at a rate of 10 °C min^{-1} from 40 to 250 °C then cooled to room temperature. Attenuated total reflectance Fourier transform infrared spectroscopy (ATR-FTIR) was acquired by a Nicolet 5700 Spectrometer. Laser scanning confocal microscope (LSCM) observations were carried out with a Nikon A1R + apparatus to examine the color tunable fluorescence property of CDs. Photoluminescence (PL) spectra was acquired by a FLS980 spectrometer with a 450 W xenon lamp. The kinetic energy harvesting and piezoelectric performance of the PVDF/CDs nanofiber were evaluated by a periodic impact apparatus.

3. Results and discussion

3.1. SEM observations

Fig. 1a illustrates the fiber preparation process, including mixing, stirring, and electrospinning. For precise investigation, different solvents constituents (DMF/Acetone: a-10/0, b-8/2, c-6/4, d-5/5) (v/v) were applied with PVDF concentration of 16% (wt/v) and electrical bias of 14 KV. Fig. S2 shows that introducing acetone as part of dual solvents could continuously improve fiber morphology with the average fiber diameters of 507, 376, 365 and 312 nm, respectively, while DMF alone is not able to provide enough conductivity and evaporation rate for fully elongation of PVDF fiber. It can be explained that the beads of higher acetone ratio could turn oval in shape and drop in number. The as collected fiber in this group has a rough distributed diameter.

Fig. S3 is the SEM results of PVDF nanofiber electrospun from different polymer concentration (a-12%, b-16%, c-20%, d-22%) (wt/v), with DMF/Acetone ratio of 5/5 (v/v) and electrical bias of 16 KV. At elevated electrical bias the fiber was thinner as expected. It is obvious to see that too low polymer concentration is not able to sustain high electrical bias so that fracture happens. As polymer concentration increases, entanglement sites between polymer chains expand and the

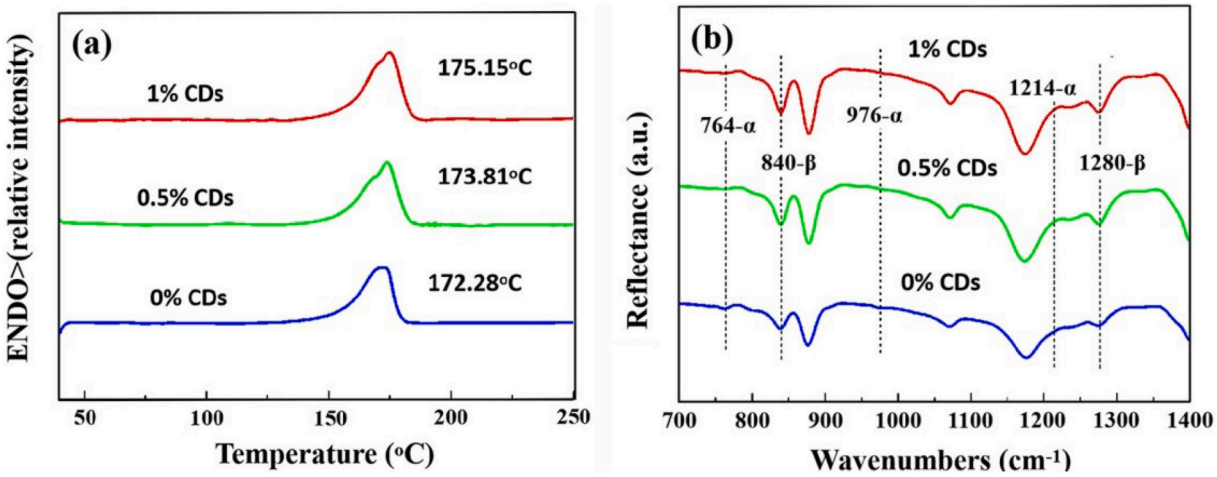

Fig. 2. DSC (a) and ATR-FTIR (b) results of PVDF nanofiber mats electrospun at 16 KV, in a mixture solvent of DMF/Acetone: 6/4 (v/v); with PVDF concentration of 20% (wt/v) and different CDs loading.

collected fiber becomes stable. However, when polymer concentration continued to increase (≥22%), conglutination occurs between fibers with fiber diameter enlarged sharply due to the fast increasing solution viscosity.

Based on above results, an electrical bias of 16 KV, a mixture of DMF/Acetone of 6/4 (v/v), and polymer concentration of 20% (wt/v) were applied for optimum fiber morphology. Herein we deprecated DMF/Acetone of 5/5 (v/v) because the spinneret blocked in real practices, Fig. 1b is the photograph of fabricated fiber mat. As can be seen in Fig. 1c, adding CDs helps decrease the average diameter of PVDF nanofiber. The average fiber diameters are 587, 395 and 406 nm for 0, 0.5 and 1% (wt/v) CDs loading, respectively. What's more, the fiber also turns more uniformly distributed with the introduction of CDs from Figs. d–f. The reason is many functional groups on CDs surfaces and better conductivity that facilitated the elongation process of PVDF fiber.

3.2. DSC and ATR-FTIR observations

Fig. 2a shows the DSC results of PVDF/CDs nanofiber mats with different CDs loading. As CDs increase from 0, 0.5–1%, the crystallinity of PVDF/CDs is improved from 9.5, 10.67–11.34%, respectively (Calculated in Supporting Information). And the melting point also shifted to a slightly higher value. Based on simplified Thomson-Gibbs equation [26], the higher melting point indicates more thermodynamic stable crystalline structures are formed in the PVDF/CDs fibers with increased CDs loading [19,25]. Also, the interaction force between polymer chains and CDs may further confine PVDF molecule movements. Thus, the melting point turns higher with increasing introduction of CDs. Moreover, from the results of ATR-FTIR in Fig. 2b, the ration of piezoelectric β crystal is improved form 85, 95–96%, respectively (Calculated in Supporting Information). Therefore, adding CDs not only enhances the whole crystallinity but facilitates the formation of β-phase crystal as well. It is also owed to the active groups on CDs' surface that acted as the nucleating agent for the crystallization behaviour in electrospun PVDF/CDs fibers.

3.3. Piezoresponse tests

Fig. 3a schematically illustrates the piezoresponse detecting apparatus. Fig. 3b depicts the charge generation process of PVDF/CDs nanofiber. Initially there is no charge on fiber surfaces. When imposed with mechanical strength, fiber mat distorts in shape. Meanwhile electrical charges of equal magnitude and opposite symbol are generated on fiber surfaces. Electrical outputs increase with the applied force. When the force is released, the signal also fades and fiber shape restores. With the same electrospinning time, the 2*2 cm^2 testing samples with 0, 0.5–1% (wt/v) CDs loading had an active layer thickness of 0.293, 0.312–0.337 mm, respectively. Fig. 3c and d reveal the short-circuit current and open-circuit voltage measured at an acceleration rate of 6 m/s^2, frequency of 1.6 Hz and applied force of 35 N. It's obvious the current and voltage enhances with an increasing ratio of CDs. In details, the maximum voltage outputs are increased from 6.4, 6.9–7.5 V, corresponding to 54.6, 55.3, and 55.6 V/cm^{-3}, respectively. The maximum current outputs are from 176.3, 225.8–286.9 nA, corresponding to 1.5, 1.8 and 2.1 $\mu A/cm^{-3}$, respectively. More interestingly, the introduction of CDs helps tailoring fiber deposition process and promotes fiber orientation toward collector. With the increase of CDs loading, thicker PVDF/CDs fiber mats are obtained with exactly the same spinning time. This further favors the enhancement of piezoelectric outputs. Compared with pure PVDF film of the same spinning time, adding 0.5% (wt/v) CDs increases the voltage output by 7.8% and current output by 28.1%, respectively. Also, adding 1% (wt/v) increases the voltage output by 17.1% and current output by 62.7%, respectively. The enhanced piezoresponse is attributed to the nucleation effect of CDs and CDs tailoring fiber deposition process.

The piezoelectric outputs of PVDF/CDs fibers at different acceleration rate is shown in Fig. 3e and f. Acceleration rate of the applied force increases from 0 to 6 m/s^2 with every increment of 0.4 m/s^2. In general, the short-circuit current and open-circuit voltage are both increased with acceleration rate. Especially at low acceleration rate (≤2.8 m/s^2), the electrical outputs are nearly linear and the slope is abrupt. At higher acceleration rate (˃ 2.8 m/s^2), the electrical outputs increase slower and start to become saturated. We attributed the saturated electrical output to the tipping point of deformation of the active layer. Therefore, the as-prepared fiber exhibits potential for acceleration sensing, especially for small acceleration changes at low frequencies [27].

Durability test was conducted for around continuous 9000 cycles and the current output remained stable (Fig. S4). We have also performed switching polarity test to ascertain true piezoelectric signals, so background noise and artifacts were ruled out of consideration, as shown in Fig. S5.

3.4. LSCM observation and PL spectrum

Fig. 4 a-c are the LSCM images of PVDF/CDs nanofiber with 1% (wt/v) CDs loading. The fibers were collected with a glass substrate for observation requirements. Fig. 4d is the PL spectrum of PVDF/CDs solution with 1% (wt/v) CDs loading. While PVDF alone shows no fluorescence, introducing CDs has endowed the composite with multifluorescence effect. As can be seen from the PL spectrum, the

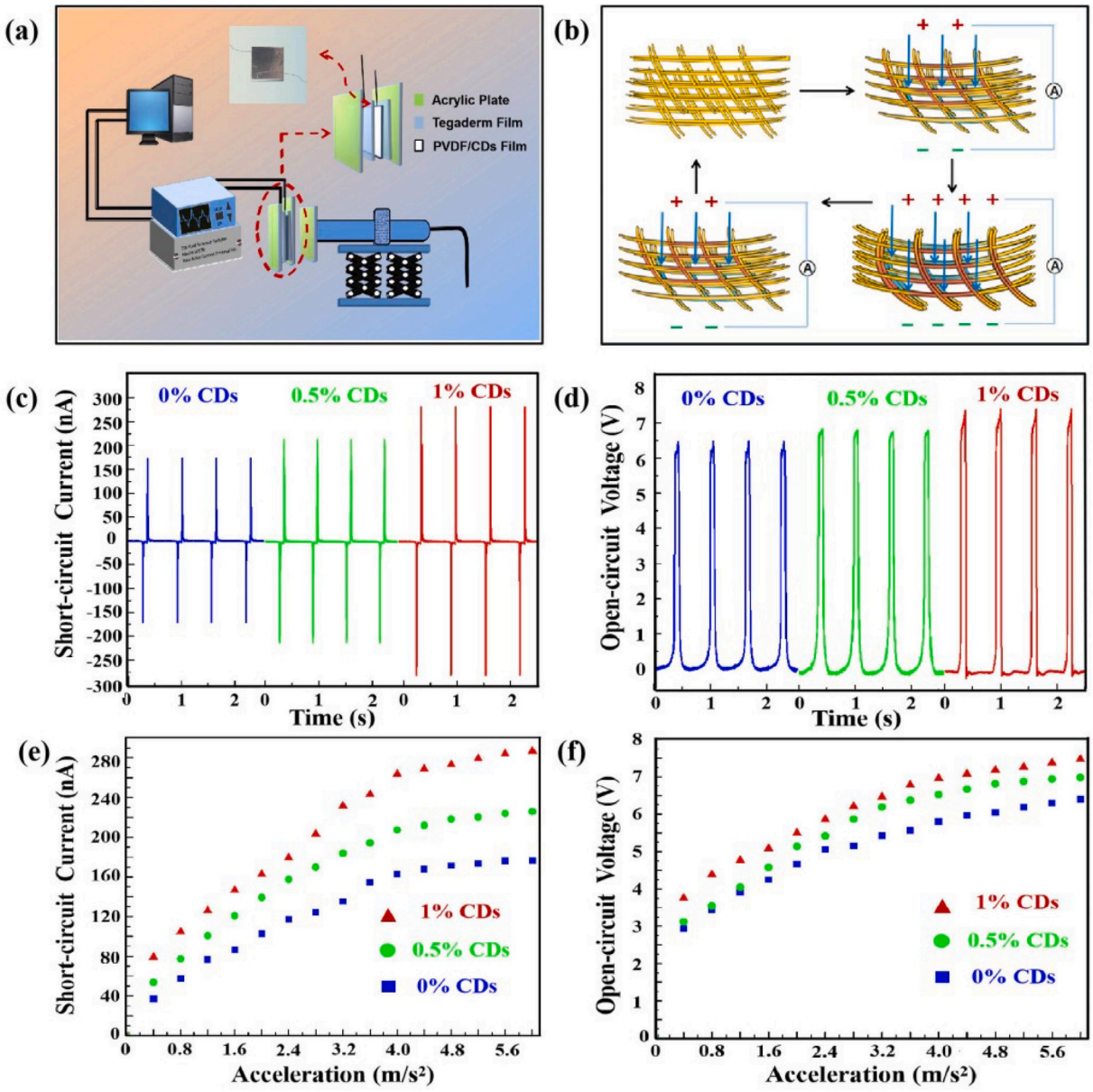

Fig. 3. (a) Illustration of piezoresponse detecting apparatus. (b) Depicts of the power generation process of PVDF/CDs nanofiber. (c–d) Current output and voltage output of PVDF/CDs fiber mats with different CDs content, measured at an acceleration rate of 6 m/s^2, frequency of 1.6 Hz and applied force of 35 N. (e–f) Current output and voltage output of electrospun PVDF/CDs fiber mats at different acceleration rate.

compound emitted different lights at different excitation wavelength. This is more directly exhibited in the LSCM images. CDs are well distributed along the fibers and emitted blue, green and red light fluorescence under the excitation of purple (405 nm), blue (488 nm) and red lights (640 nm), respectively. These results demonstrate the excitation-light dependent tunable luminescence of PVDF/CDs electrospun fibers.

4. Conclusion

In summary, PVDF/CDs nanofiber mats were prepared for the first time with a conventional needle based electrospinning setup. The introduction of CDs tailored the spinning deposition process, reduced fiber diameter, facilitated the formation of piezoelectric crystalline β phase, and endowed the hybridized nanofibers with color tunable fluorescence. In particular, the electrical outputs of PVDF/CDs nanofibers were very sensitive to small acceleration changes at low frequency. At an acceleration rate of 6 m/s^2, frequency of 1.6 Hz and applied force of 35 N, the PVDF/CDs nanofiber delivered the maximum open-circuit voltage density of 55.6 V cm^{-3}, and short-circuit current density of 2.1 μA cm^{-3}, respectively. We believe this work would be beneficial to the development of novel piezoelectric nanofibrous materials that promise applications in a new generation of self-powered autonomous optoelectronic devices.

Declaration of competing interest

The authors declare that they have no known competing financial interests or personal relationships that could have appeared to influence the work reported in this paper.

CRediT authorship contribution statement

Xi Huang: Methodology, Validation, Investigation, Writing - original draft. **Long Jin:** Investigation, Writing - review & editing. **Chuanfeng Wang:** Investigation. **Yali Xu:** Investigation. **Zhou Peng:** Investigation. **Meilin Xie:** Investigation. **Chaoliang Zhang:** Investigation. **Weiqing**

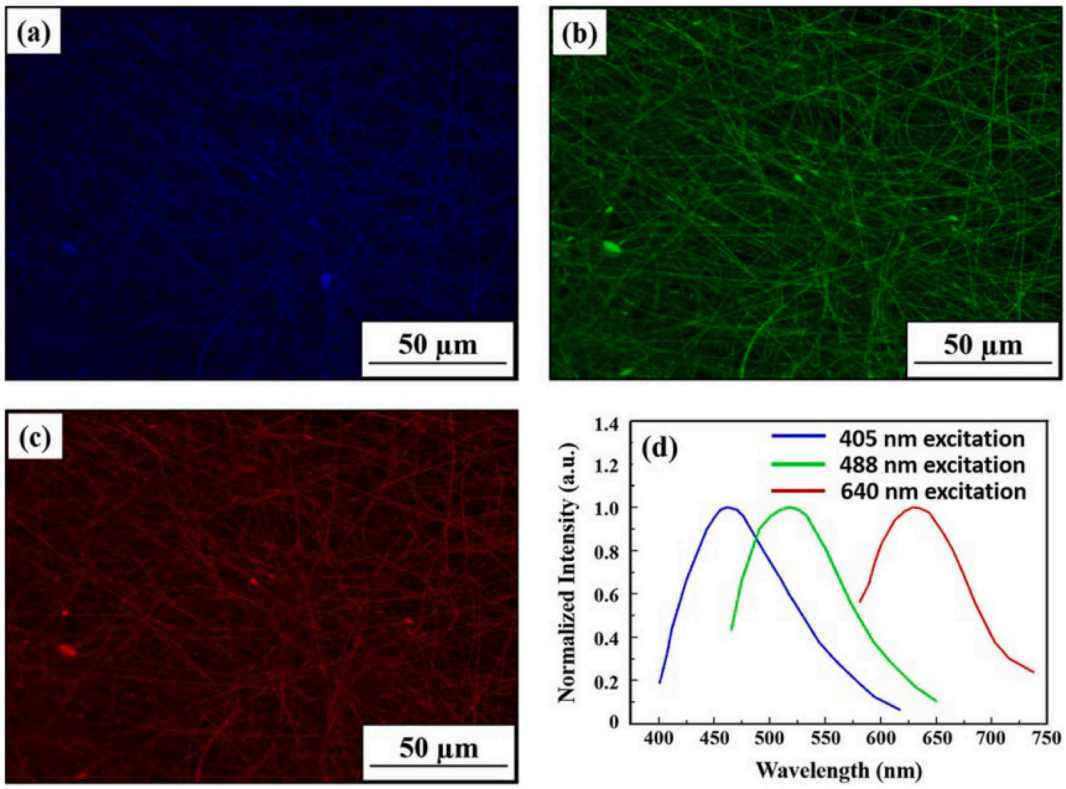

Fig. 4. (a–c) LSCM images of PVDF/CDs nanofibers with 1% (wt/v) CDs loading, excited under light wavelength of 405, 488 and 640 nm, respectively. (d) PL spectrum of PVDF/CDs solution with 1% (wt/v) CDs loading.

Yang: Resources, Supervision. **Jun Lu:** Conceptualization, Resources, Supervision, Funding acquisition.

Acknowledgements

This work is supported by Sichuan Science and Technology Program (No. 2018JY0166) and National Natural Science Foundation of China (No. 51373139).

Appendix A. Supplementary data

Supplementary data to this article can be found online at https://doi.org/10.1016/j.coco.2020.04.014.

References

[1] Z.L. Wang, Entropy theory of distributed energy for internet of things, Nano Energy 58 (2019) 669–672.
[2] W. Wang, Y. Wu, Z. Chang, F. Chen, H. Wang, G. Gu, H. Zheng, G. Cheng, Z. L. Wang, Self-powered intelligent water meter for electrostatic scale preventing, rust protection, and flow sensor in a solar heater system, ACS Appl. Mater. Interfaces 11 (2019) 6396–6403.
[3] R. Saraf, L. Pu, V. Maheshwari, A light harvesting, self-powered monolith tactile sensor based on electric field induced effects in $MAPbI_3$ perovskite, Adv. Mater. 30 (2018) 201705778.
[4] C. Kumar, A. Gaur, S. Tiwari, A. Biswas, S.K. Rai, P. Maiti, Bio-waste polymer hybrid as induced piezoelectric material with high energy harvesting efficiency, Compos. Commun. 11 (2019) 56–61.
[5] T. Hanashi, T. Yamazaki, H. Tanaka, K. Ikebukuro, W. Tsugawa, K. Sode, The development of an autonomous self-powered bio-sensing actuator, Sensor. Actuator. B Chem. 196 (2014) 429–433.
[6] C.W. Xu, L. Zhang, Y.L. Xu, Z.Z. Yin, Q. Chen, S.Y. Ma, H.H. Zhang, R. Huang, C. L. Zhang, L. Jin, W.Q. Yang, J. Lu, Filling the holes in piezopolymers with a solid electrolyte: a new paradigm of poling-free dynamic electrets for energy harvesting, J. Mater. Chem. A 5 (2017) 189–200.
[7] H.J. Kim, J.H. Kim, K.W. Jun, J.H. Kim, W.C. Seung, O.H. Kwon, J.Y. Park, S. W. Kim, I.K. Oh, Silk nanofiber-networked bio-triboelectric generator: silk bio-TEG, Adv. Energy Mater. 6 (2016) 1502329.
[8] Z. Lin, J. Chen, X. Li, Z. Zhou, K. Meng, W. Wei, J. Yang, Z.L. Wang, Triboelectric nanogenerator enabled body sensor network for self-powered human heart-rate monitoring, ACS Nano 11 (2017) 8830–8837.
[9] L. Jin, B.B. Zhang, L. Zhang, W.Q. Yang, Nanogenerator as new energy technology for self-powered intelligent transportation system, Nano Energy 66 (2019) 104086.
[10] L. Jin, J. Chen, B.B. Zhang, W.L. Deng, L. Zhang, H.T. Zhang, X. Huang, M.H. Zhu, W.Q. Yang, Z.L. Wang, Self-powered safety helmet based on hybridized nanogenerator for emergency, ACS Nano 10 (2016) 7874–7881.
[11] Q. Qiu, M.M. Zhu, Z.L. Li, K.L. Qiu, X.Y. Liu, J.Y. Yu, B. Ding, Highly flexible, breathable, tailorable and washable power generation fabrics for wearable electronics, Nano Energy 58 (2019) 750–758.
[12] Y. Hu, Z.L. Wang, Recent progress in piezoelectric nanogenerators as a sustainable power source in self-powered systems and active sensors, Nano Energy 14 (2015) 3–14.
[13] B. Ameduri, From vinylidene fluoride (VDF) to the applications of VDF-containing polymers and copolymers: recent developments and future trends, Chem. Rev. 109 (2009) 6632–6686.
[14] S. Sankaranarayanan, J. Hermosilla, F. Acevedo, R. Navia, The influences of solvents on the electrospun of whole Scenedesmus almeriensis and poly(ethylene oxide) for the preparation of composite nanofibers, Compos. Commun. 10 (2018) 18–24.
[15] F.L. Lai, D.Y. Yong, X.L. Ning, B.C. Pan, Y.E. Miao, T.X. Liu, Bionanofiber assisted decoration of few-layed $MoSe_2$ nanosheets on 3D conductive networks for efficient hydrogen evolution, Small 13 (2017) 1602866.
[16] Y. Zhu, M. Yin, H.S. Liu, B. Na, R.H. Lv, B. Wang, Y.H. Huang, Modification and characterization of electrospun poly (vinylidene fluoride)/poly (acrylonitrile) blend separator membranes, Compos. B Eng. 112 (2017) 31–37.
[17] H. Shao, J. Fang, H. Wang, T. Lin, Effect of electrospinning parameters and polymer concentrations on mechanical-to-electrical energy conversion of randomly-oriented electrospun poly(vinylidene fluoride) nanofiber mats, RSC Adv. 5 (2015) 14345–14350.
[18] R. Guo, H. Luo, W.W. Liu, X.F. Zhou, L. Tang, K.C. Zhou, D. Zhang, High energy density in PVDF nanocomposites using an optimized nanowire array, Phys. Chem. Chem. Phys. 20 (2018) 18031–18037.
[19] J.H. Yu, P.K. Jiang, C. Wu, L.C. Wang, X.F. Wu, Graphene nanocomposites based on poly (vinylidene fluoride): structure and properties, Polym. Compos. 32 (2011) 1483–1491.
[20] Y. Zhou, S. Chen, D. Wu, L. Liu, H. Luo, D. Zhang, Enhanced dielectric properties of poly(vinylidene fluoride-co-hexafluoropropylene) nanocomposites using oriented nickel nanowires, Compos. Commun. 16 (2019) 11–19.
[21] X.J. Zha, J.H. Pu, L.F. Ma, T. Li, R.Y. Bao, L. Bai, Z.Y. Liu, M.B. Yang, W. Yang, A particular interfacial strategy in PVDF/OBC/MWCNT nanocomposites for high dielectric performance and electromagnetic interference shielding, Compos. Part A-Appl S 105 (2018) 118–125.

[22] X. Yuan, W. Li, H. Liu, N. Han, X. Zhang, A novel PVDF/graphene composite membrane based on electrospun nanofibrous film for oil/water emulsion separation, Compos. Commun. 2 (2016) 5–8.
[23] Z.H. Sun, Z.Q. Yan, R. Yin, X.S. Huang, K.C. Yue, A.R. Li, L. Qian, Homogeneous poly(vinylidenefluoride)-graphene films with secondary percolation behaviors towards negative permittivity properties, Compos. Commun. 17 (2020) 18–21.
[24] S.Y. Ma, L. Jin, X. Huang, C. Riziotis, R. Huang, C.L. Zhang, J. Lu, W.Q. Yang, Nanogenerators begin to light up: a novel poling-free piezoelectric system with multicolor photoluminescence as an efficient mechatronics development platform, Adv. Mater. Interfaces 5 (2018) 1800587.
[25] X.B. He, C.F. Wang, X. Huang, L. Jin, X. Chu, M.L. Xie, Y.W. Nie, Y.L. Xu, Z. Peng, C.L. Zhang, J. Lu, W.Q. Yang, Carbon nanolights in piezopolymers are self-organizing toward color tunable luminous hybrids for kinetic energy harvesting, Small 16 (2020) 1905703.
[26] B. Wunderlich, Macromolecular physics, in: Crystal Structure, Morphology, Defects, vol. 1, Academic Press, New York, 1973.
[27] L. Jin, S.Y. Ma, W.L. Deng, C. Yan, T. Yang, X. Chu, G. Tian, D. Xiong, J. Lu, W. Q. Yang, Polarization-free high-crystallization β-PVDF piezoelectric nanogenerator toward self-powered 3D acceleration sensor, Nano Energy 50 (2018) 632–638.